Fibers and Polymers 2016, Vol.17, No.3, 311-323
DOI 10.1007/s12221-016-5361-y

ISSN 1229-9197 (print version)
ISSN 1875-0052 (electronic version)

A Novel Biodegradable Polyurethane Based on Hydroxylated Polylactic Acid and Tung Oil Mixtures. I. Synthesis, Physicochemical and Biodegradability Characterization

Hossein Izadi-Vasafi*, Gity Mir Mohamad Sadeghi[1], Amir Babaei[2], and Faezeh Ghayoumi

Department of Polymer Engineering, Shahreza Branch, Islamic Azad University, Shahreza 86145-311, I. R. Iran
[1]Department of Polymer Engineering and Color Technology, Amirkabir University of Technology, Tehran 15875-4413, I. R. Iran
[2]Polymer Engineering Department, Faculty of Engineering, Golestan University, Gorgan 49188-88369, I. R. Iran
(Received May 11, 2015; Revised January 18, 2016; Accepted February 10, 2016)

Abstract: A novel biodegradable polylactic acid-based polyurethane (PU) was synthesized via a chain extension reaction between hydroxylated polylactic acid (PLA-OH) and hydroxylated tung oil (HTO) using 1,6-hexamethylene diisocyanate (HDI) to link the two polyols and dibutyltin dilaurate (DBTDL) as a catalyst. Both PLA-OH and HTO, as polyols, were separately synthesized in our laboratory. Three different molecular weights of PLA-OH prepolymers were used, and the molar ratio of PLA-OH to HTO was also changed to investigate the effect of these two parameters on the structure and properties of the final PUs. Chemical structures of PLA-OH, HTO, and final PUs were investigated by Fourier transform infrared (FTIR) and Hydrogen-1 nuclear magnetic resonance (^{1}HNMR) spectroscopies. Thermal transitions and thermal stability of the final PUs were, respectively, studied by differential scanning calorimetry (DSC) and thermogravimetric analysis (TGA). The FTIR and ^{1}HNMR results showed that the chain-extension reaction of the two polyols with HDI was sufficiently achieved. The TGA results showed that the polyurethanes based on the lower molecular weight PLA segments were more thermally stable; it was not degraded up to 270 °C. DSC results showed that incorporating HTO in the PU chains led to formation of more flexible PU chains, while the glass transition temperatures of the PUs of higher PLA-OH molecular weights were higher than those of lower ones.

Keywords: Biodegradable, Polylactic acid, Hydroxylated tung oil, Polyurethane

Introduction

Application of biopolymers in both biomedical and general commodity products is increasingly obvious in academic and industrial environments nowadays and growing attention has being paid to these materials to extend their applications [1-4]. Polylactic acid (PLA) is one of the major members in the family of biodegradable and biocompatible polymers. Beside its application as a biopolymer in the field of medical application, such as drug delivery [5,6], sutures [7,8], implants [9], and tissue engineering [10,11], its monomer, lactic acid (LA), can be used for preparing telechelic prepolymers to synthesize biodegradable polyurethanes [12-15]. Since one of the major limitations of PLA regarding its mechanical properties is its brittle behavior and poor toughness, various methods have been explored to toughen PLA, such as blending with some elastomeric or tough polymers, copolymerizing of LA with flexible polymers, or chain extension reaction of PLA prepolymer with flexible prepolymer chains [14,15]. A common approach for toughening PLA is using a flexible monomer or macromolecule to copolymerize with LA to synthesize PLA-based random or block copolymers [13,16-18]. For instance, Borda *et al*. [13] obtained PLA-based polyurethanes and reported the optimum reaction conditions (such as reaction time, reaction temperature, molar ratios, and catalyst) on the molecular weight of this kind of linear polyurethanes. However, they did not study the effect of prepolymer molecular weight on the structure and thermal properties of their PLA-based polyurethanes. For multiblock copolymers, such as poly(l-lactic acid) – polycaprolactone [16], poly(l-lactic acid) – poly(ethyelene glycol) [17], poly(l-lactic acid) – poly(trimethylene carbonate [18], etc., high molecular weights could be achieved along with good mechanical properties.

In the case of chain-extension reactions of PLA prepolymer with a flexible prepolymer in the presence of a chain extender, typical biodegradable PLA-based polyurethane can be synthesized which could yield a variety of materials having a wide range of properties, from thermoplastics to elastomers. During the last two decades many flexible prepolymers, such as poly(ethylene oxide) [19], poly(ethylene glycol) [20], poly(ε-caprolactone) [21,22], etc., have been added to the PU formulation as a flexible component.

Tung oil (TO), also called as China wood oil, is a vegetable oil obtained from the seeds or nuts of the tung tree [23]. The major component of this oil is α-eleostearic acid (77-82 %) which has three conjugated double bonds in its molecule structure, while the other components include oleic acid (3.5-12.7 %) with one double bond, linoleic acid (8-10 %) with three non-conjugated double bonds, and palmitic acid (3-5 %) which is a saturated fatty acid [24]. The carbon-

*Corresponding author: hizadi@iaush.ac.ir

carbon double bonds of these fatty acids can act as reactive sites and react with other chemicals to obtain an intermediate product for making other materials, like polymers [25]. For example, natural polyols can be obtained by hydroxylation or alcoholysis reaction of the double bonds along a fatty acid chain, introducing hydroxyl groups to the oil structure. During the last two decades some attempts have been done to synthesize oil-based polyurethanes and to characterize the corresponding PU [26-30]. However, to our knowledge, synthesis of polyurethane based on hydroxylated PLA (PLA-OH) and hydroxylated tung oil (HTO) has not been described yet. In the work by Borda *et al*. [13], only the effect of reaction parameters on the molecular weight of the linear polyurethanes were demonstrated, with some of these conditions being optimized; however, the thermal transitions of the PLA-based polyurethanes (thermal stability and thermal properties) were not studied. Mosiewicki *et al*. [30] synthesized polyurethanes from a polyol based on tung oil and studied the reinforcement of the resulting polyurethanes with wood flour and microcrystalline cellulose. According to our literature review, it was clear that no work has been reported on the synthesis and characterization of biodegradable polyurethane based on mixtures of hydroxylated PLA (PLA-OH) and hydroxylated tung oil (HTO).

In this study, we investigated the synthesis of a novel PU based on PLA-OH and HTO. These two polyols were prepared in our laboratory. The chemical structure, and also the thermal properties, of the final PUs were investigated and the effect of PLA-OH molecular weight and molar ratio of PLA-OH to HTO on the structure and thermal properties of the final PUs were investigated.

Experimental

Materials

Hydroxylated polylactic acid (PLA-OH) was prepared in our laboratory. Its preparation route has been described elsewhere by the authors [31]. For synthesis of PLA-OH, L-Lactic acid (LA) (88 % L-lactic acid in water, 99 % optically pure) was purchased from Sigma Chemical Co., USA. The excess water was removed before use by distillation under reduced pressure at 85 °C. Tung oil (specific gravity of 0.93 g/cm^3, saponification value equal to 195 mg KOH/g, acid value equal to 2.1 mg KOH/g) was purchased from Ariaresin Co., Iran. Hydrogen peroxide (30 wt%) from Dr. Mojallali Laboratories, Iran, and formic acid (88 wt%) from Merck, Germany, were used in the hydroxylation reaction of TO. Before reaction, the accurate formulation of the hydrogen peroxide was measured by a titration procedure; 28 wt% was obtained. 1,6-hexamethylene diisocyanate (HDI) from Merck, Germany, for linking two polyols together, and dibutyltin dilaurate (DBTDL), from Sigam-Aldrich, USA, as the catalyst were used as received.

Synthesis of Tung Oil-based and Polylactic Acid-based Polyols

HTO was synthesized by hydroxylation of TO similar to the procedure described by Mosiewicki *et al*. [30]. Predetermined amounts of hydrogen peroxide and formic acid solutions were added to a glass reactor and the reactor was immersed in a water bath having a temperature of 40 °C. After mixing the reactant by a mixer, the pure tung oil was added dropwise to the mixture and the temperature was kept between 40 and 50 °C for 3 h. In this step, the initial ratio of oil/H_2O_2 (by weight) was equal to 3.5/1 and H_2O_2/HCOOH (by weight) equal to 1/1.9. After 3 hours, the product was cooled down to room temperature. The liquid separated clearly into two phases. The lower layer (which was an acidic solution) was removed and the upper layer (which contained HTO) was recovered and distilled under vacuum to eliminate remaining water and acid.

PLA-OH was also synthesized in our laboratory. Its preparation route was described in a previous report [31]. In order to investigate the effect of PLA-OH molecular weight on the structure and properties of the final PUs, three different molecular weights (1100, 1650, and 2200 g/mol) of PLA-OH samples were chosen. More details about these molecular weights are discussed in the Results and Discussion section.

Before the synthesis of PUs, both polyols were placed in a vacuum oven (60 °C overnight) to remove any potential water.

Polyurethane Synthesis (chain-extension reaction)

Three different molecular weights of PLA-OH along with HTO were used to synthesize the final PU samples. Table 1 shows the different PLA-OH molecular weights and feed compositions for synthesis of the final PU samples. For synthesis of all samples, the molar ratio of NCO to OH was

Table 1. Feed composition of polyols for PU synthesis

Samples	PLA-OH MW	PLA-OH (mol%)	HTO (mol%)
P1-100-0	1100	100	0
P1-75-25	1100	75	25
P1-50-50	1100	50	50
P1-25-75	1100	25	75
P2-100-0	1650	100	0
P2-75-25	1650	75	25
P2-50-50	1650	50	50
P2-25-75	1650	25	75
P3-100-0	2200	100	0
P3-75-25	2200	75	25
P3-50-50	2200	50	50
P3-25-75	2200	25	75

set to 1:1. The OH values of both kinds of polyols are also shown in Table 1.

The chain-extension reaction of both polyols was performed in a glass reactor under nitrogen atmosphere. PLA-OH and HTO, along with a few drops of DBTDL, were added to the reactor. Then the reactor was immersed in a 100 °C silicone oil bath. The reactants were stirred mechanically, becoming completely molten after about 1 min. Then a predetermined amount of HDI was added dropwise to the mixture. The chain-extension reaction was finished in 1 hour, during which time nitrogen fed into the reaction vessel. At the end of the reaction, the molten product was poured into a mold and allowed to cool down to room temperature before characterization.

Characterization of PLA-OH, HTO, and Polyurethanes

Fourier transform infrared (FTIR) spectroscopy was performed with a PerkinElmer 65 (USA) FTIR spectrometer (resolution 8.0 cm^{-1}, number of scans equal to 5) to identify the chemical structures of the PLA-OH, TO, HTO, and final PU samples.

To insure the molecular structure of the products, nuclear magnetic resonance (NMR) spectra were also recorded, on a Bruker 500 NMR spectrometer, Germany, with deuterated chloroform as the solvent.

The number average molecular weight (M_n), weight average molecular weight (M_w) and polydispersity index (PDI) of the polyurethanes were determined by gel permeation chromatography (GPC, Agilent 1100 series, USA; the column was calibrated with polystyrene standards, the solvent was $CHCl_3$, temperature was set to 30 °C, and flow rate was 1 ml/min).

For thermal analysis of all samples, differential scanning calorimetry (DSC) analysis was implemented on a Perkin Elmer Instrument DSC Diamond (USA). The PU samples were slowly cooled to -60 °C and then heated to 110 °C at a rate of 10 °C/min. The crystallinity of the PUs was calculated by the following equation:

$$Crytallinity \text{ Percent } (\%X_C) = \frac{\Delta H_m}{\Delta H_m^{\infty}} \times 100$$

where ΔH_m is the enthalpy of melting, and ΔH_m^{∞} is the enthalpy of melting of ideally crystalline PLA (94 J/gr) [3]; In fact, the crystallization of PUs was compared to that of the PLA in our study. The reason is that, because the PU samples were synthesized for the first time, so no data was available for them. Therefore, considering that only PLA segments crystallize on the PUs, we chose the data of pure PLA.

Thermogravimetric analysis (TGA) was used to recognize the thermal stability of the final PU samples. The corresponding thermograms were recorded on a Perkin Elmer Pyris1 instrument from room temperature to 500 °C at a heating rate of 10 °C/min under nitrogen atmosphere.

The biodegradation test of the PU samples was carried out using simulated body fluid (SBF). The general SBF used in our study was a buffer solution with pH around 7.4. It contains ultra-pure water, sodium chloride, sodium hydrogen carbonate, potassium chloride, hydrogen chloride, and some other salts. The samples were placed in SBF in an incubator for 15 days. After this period of time the samples were taken out, placed under nitrogen and, subsequently, vacuum overnight until a constant weight was reached. The samples were weighed before and after being placed in the SBF, with the weight loss being obtained using the following formula:

$$Weight\ loss\ (\%) = \frac{m_0 - m_t}{m_0} \times 100$$

in which m_0 is the initial (pre-degraded) weight of the dry sample and m_t is the dry weight of the sample after placing in SBF. This weight loss was chosen as a biodegradation criterion for the synthesized PUs.

Results and Discussion

Chemical Structure of PLA-OH (FTIR and ^{1}HNMR results)

The PLA-OH prepolymers were synthesized by direct condensation polymerization of L-lactic acid in the presence of 1,4-butaendiol using tin(II) octoate as a catalyst (Scheme 1). The FTIR spectrum of a PLA-OH sample (molecular weight of 2200 g/mol) is shown in Figure 1. The peaks occurring at 3400 cm^{-1} is related to the -OH group at the end of the prepolymer chains.

As mentioned earlier, PLA-OH samples with three different molecular weights were synthesized in our work. The FTIR spectra of all samples were similar to each other, so the structure and the groups of all three samples were the same, as in our previous study [31].

Figure 2 shows the ^{1}HNMR spectrum of the PLA-OH sample along with the chemical structure and the corresponding chemical shifts of its protons [14]. The different chemical shifts for the PLA-OH chain is shown inside Figure 2.

The average degree of polymerization (DP_n) and the number average molecular weights ($M_{n,NMR}$) of the PLA-OH samples can be calculated from ^{1}HNMR spectroscopy of the

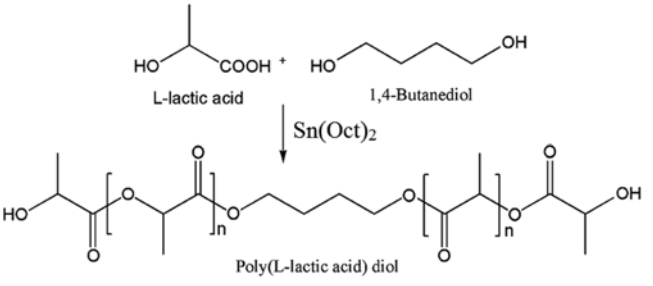

Scheme 1. Process route for synthesis of PLA-OH.

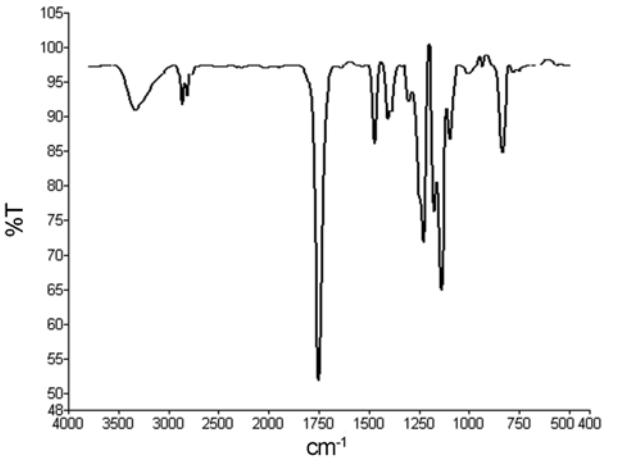

Figure 1. FTIR spectrum of PLA-OH sample.

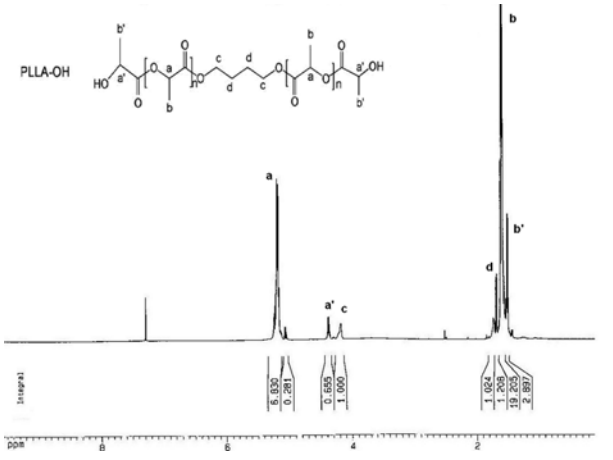

Figure 2. Chemical structure of PLA-OH and the corresponding HNMR chemical shifts.

samples according to the following equations (equation (1) and (2)) [14]:

$$DP_n = 2 \times \frac{I_{5.18} + I_{4.36}}{I_{4.36}} \quad (1)$$

$$M_n = 72 \times DP_n + 88 + 2 \quad (2)$$

where $I_{5.18}$ and $I_{4.36}$ are the intensities of the peaks related to methine groups in the interior and ends of the PLA-OH chains, respectively. The factor 2 in equation (1) indicates the two identical chain segments on both sides of $-OCH_2CH_2CH_2CH_2O-$, and the numerical values of 72, 88, and 2 are, respectively, the molecular weights of the repeating units of the PLA chains, the residue of 1,4-BDO inside the chain, and the mass of the two proton hydrogens at the PLA-OH chain ends.

It should be noted that in this study $M_{n,NMR}$ was used for calculation in the synthesis of final PUs, because it was proved by some literature work [32-34] that this parameter was very effective to determine the amount of diisocyanate. According to the reaction parameters in our experiment, the three samples with molecular weights of 1100, 1650, and 2200 g/mol were selected for the PU synthesis [31].

Chemical Structure of HTO (FTIR and ^{1}HNMR results)

In the case of hydroxylated tung oil (HTO), after the modification of TO and reaction with the solution of hydrogen peroxide and formic acid, its viscosity increased and it became a paste-like material along with a color change. The increase of viscosity resulted from the introduction of hydroxyl groups to the pure (unmodified) TO and, subsequently, some intermolecular H-bond interactions. As proposed by Hu *et al*. [28], reaction of hydrogen peroxide with formic acid leads to the formation of performic acid. By adding tung oil to the mixture, the carbon-carbon double bonds in the fatty acids undergo an intermediate process of epoxidation. Finally, because of the strong acid conditions of the media, the epoxide groups would be very unstable and open to form hydroxyl groups. Scheme 2 shows the overall hydroxylation reaction of TO [28]. The hydroxyl value of HTO was 250 mg KOH/g, while TO has essentially no hydroxyl groups in its structure.

Figure 3 shows the FTIR spectrum of TO and HTO. In Figure 3(a), no clear peak can be seen at around the 3400 cm^{-1} region, while broad peak at this region is clear in Figure 3(b), indicating that OH groups existed in the HTO structure. On the other hand, the peak at 3010 cm^{-1} in Figure 3(a) related to -CH=CH- unsaturated bonds, was not present in Figure 3(b). Another point is that, the intensity of the peak at 991 cm^{-1} in Figure 3(b) (which is assigned to the movement of conjugated unsaturated bonds in eleostearic acid) was much weaker than that in Figure 3(a), indicating that a considerable decrease in unsaturated bonds concentration happened during the hydroxylation reaction. The above mentioned reasons showed that the hydroxylation reaction of tung oil was done well and most of the double bonds in its structure were converted into the hydroxyl groups [30].

It should be noted here that our hydroxylation of TO was similar to the procedure described by Mosiewicki *et al*. [30];

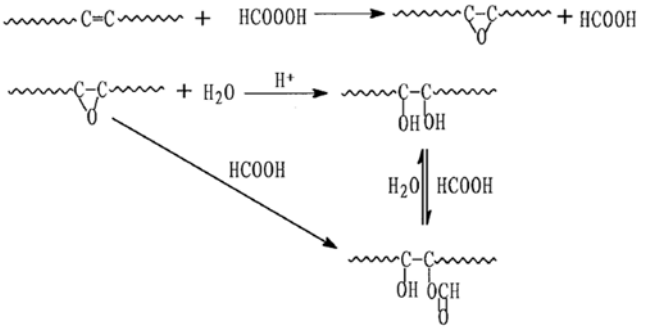

Scheme 2. Overall hydroxylation process of pure tung oil.

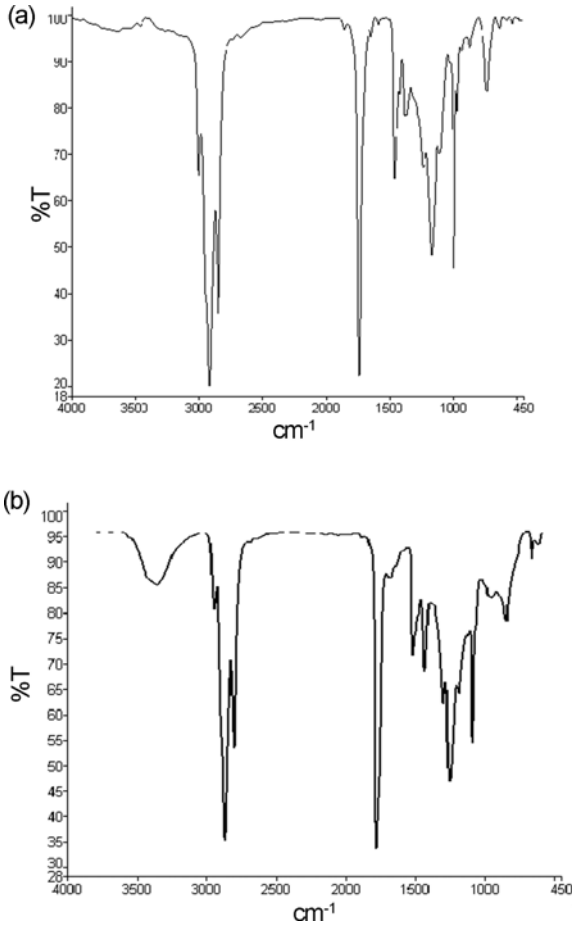

Figure 3. FTIR spectrum of (a) pure tung oil and (b) hydroxylated tung oil.

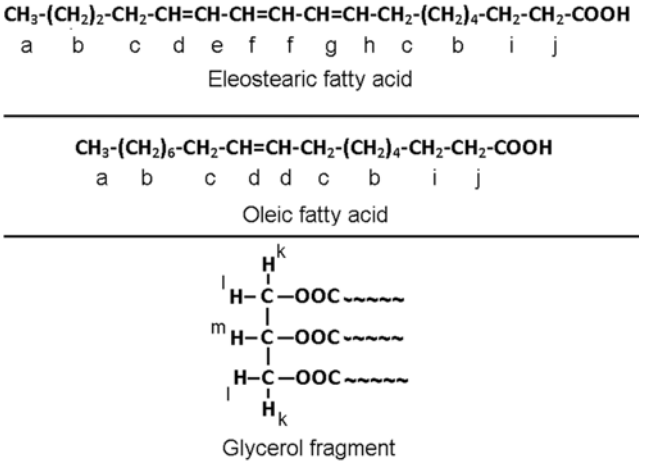

Scheme 3. The structure of eleostearic and oleic acid in TO.

however, the aim of our study was only to hydroxylate TO, not to alcoholize it. So the concentration of OH groups was not very high and, as a result, the intensity of the peak at 3400 cm^{-1} was not very high. In the study by Mosiewicki *et al*. [30], the intensity of this peak became stronger after the alcoholysis reaction.

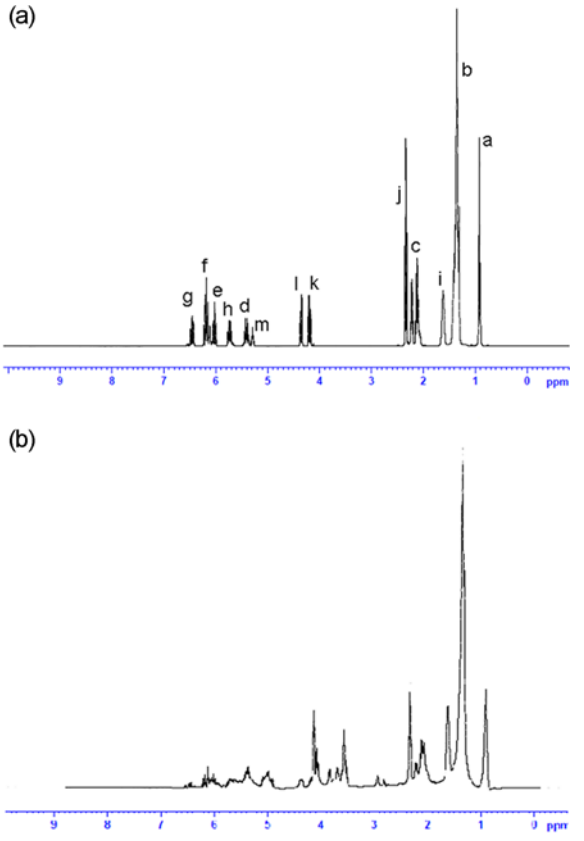

Figure 4. ^{1}HNMR spectrum of (a) pure tung oil, (b) hydroxylated tung oil, related to two major fatty acids of it.

To verify the FTIR results, ^{1}HNMR analysis of TO and HTO was also done in our study. Considering the simple assumption that the major fatty acids present in TO are eleostearic and oleic acids, the structures of these two fatty acids are shown in Scheme 3 and the chemical shifts assigned to the corresponding protons are shown in Figure 4(a). The different peaks and the corresponding hydrogens can be seen by comparing Scheme 3 and Figure 4(a).

The ^{1}HNMR spectrum of HTO is shown in Figure 4(b). Comparing the ^{1}HNMR spectra of TO and HTO, the following differences and results can be recognized:

- The intensity of the four sets of multiplet shifts between 5.4 and 6.5 ppm in Figure 4(a) (g, f, e, h) related to the unsaturated protons (vinyl hydrogens) along the eleostearic and oleic acid structures, bacame considerably weaker in Figure 4(b), indicating the decrease of unsaturated bonds concentration after the hydroxylation reaction of TO.
- The appearance of a rather broad peak at 4.7-5.2 ppm and also the peaks at 3.52-3.85 ppm in Figure 4(b) (which are not present in Figure 4(a)) correspond to the hydroxyl protons along the fatty acid chains as a result of hydroxylation.

Based on the FTIR and ^{1}HNMR results, we concluded that hydroxylation of TO was successfully done and that the hydroxyl groups were attached to the backbone of the fatty acid chain.

It should be noted that in our study we simply assumed that TO would be a diol for the synthesis of PU, i.e. only two chains of its three-chain-triglyceride would have hydroxyl group after hydroxylation reaction. Considering this hypothesis, the molecular weight of HTO was assumed equal to 400 g/mol for its mole percent determination in the calculation during formulation of final PU synthesis.

Chemical Structure of Final Synthesized PUs (FTIR and ^{1}HNMR results)

First, the solubility of synthesized PU in chloroform was evaluated; and the experiment showed that all synthesized PUs dissolved with no remaining gel content. Furthermore, the synthesized PUs had melting points around 100 °C (which was verified by DSC). These two results showed that all synthesized PUs had linear structures, being neither crosslinked nor network and, consequently, we came to the conclusion that HTO preferentially acted as a diol, not a triol.

Also, the hydroxyl values of some of the PLA-OH samples were measured (according to ASTM D4274) and the correlation with the ^{1}HNMR molecular weights was verified.

Thus, the proposed structure of the final synthesized PUs is shown in Scheme 4. As shown in the scheme, the two polyols used in this study were the soft segments and the urethane bonds along with the HDI component were the hard segments (HS).

Figure 5(a) shows the FTIR spectrum of the P3-100-0 sample, for synthesis of which, no TO was used. No clear absorption peak can be seen at 2270 cm^{-1} (related to -N=C=O group), indicating that almost all of the isocyanate groups of the HDI disappeared during the reaction of PLA-OH. On the

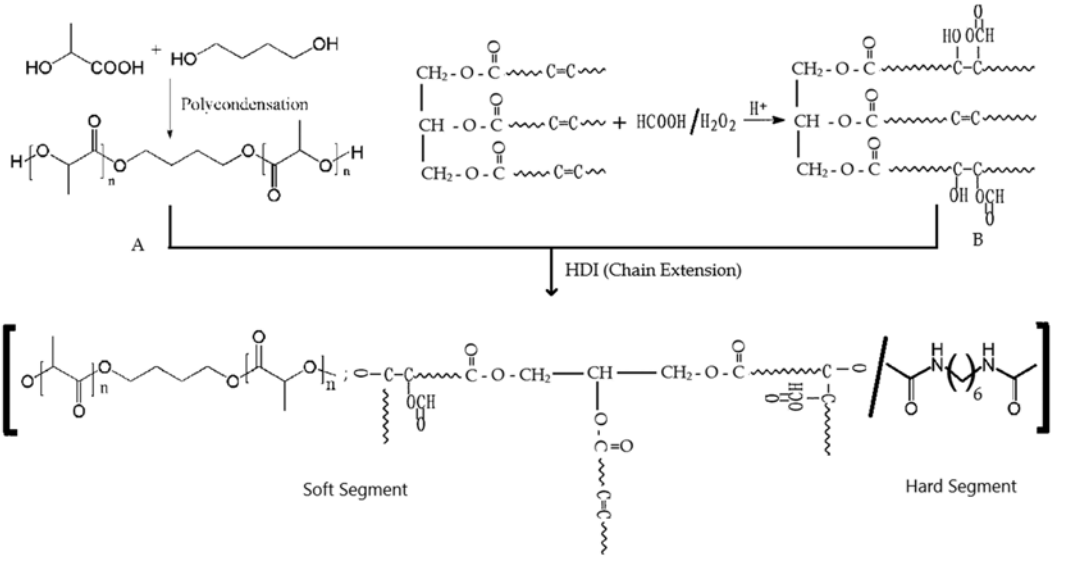

Scheme 4. The proposed structure of the final synthesized PU.

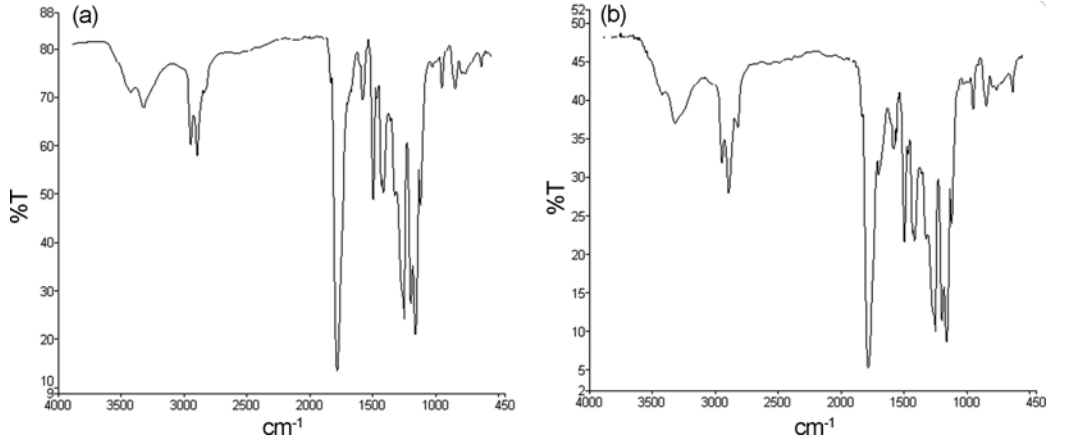

Figure 5. FTIR spectrum of (a) P3-100-0 sample and (b) P3-50-50 sample.

other hand, the stretching peaks at 1750-1630 cm^{-1} region (-C=O of urethane bond) and also 3500-3200 cm^{-1} (-NH of urethane bond) can be seen in Figure 5(a), which confirmed the formation of urethane linkage. The FTIR spectrum of the P3-50-50 sample is shown in Figure 5(b). For this synthesized PU, the mole ratio of PLA-OH to HTO was 0.50:0.50. There was also no absorption peak at 2270 cm^{-1} for this synthesized PU. It has been shown that the infrared absorbance of the H-bonded urethane carbonyl groups appears at lower wavenumbers than that of free urethane carbonyls [35]. As seen in Figure 5(b), a poor but clear peak occurred at 1667 cm^{-1} near 1755 cm^{-1} peak, indicating that there were some N-H bending and hydrogen-bonded carbonyl groups, respectively, in this synthesized PU. Thus, we concluded that hydrogen bonds existed in the PU samples containing HTO in their structure. In the case of the -NH stretching band, the hydrogen-bonded -NH groups and non-hydrogen-bonded -NH groups showed absorption peaks at 3330-3320 cm^{-1} and 3445-3390 cm^{-1}, respectively. In Figure 5(b), a small peak can be observed at 3395 cm^{-1}, which indicates that the amount of non-hydrogen bonded -NH groups were more than that of the hydrogen bonded -NH groups. Other absorption peaks in the PU samples were similar to the ones in the corresponding polyols. We note that, the FTIR spectrum of the other samples which did not have any HTO in their composition were similar to that of P3-100-0, and samples which had HTO in their compositions were similar to P3-50-50; so they are not shown here.

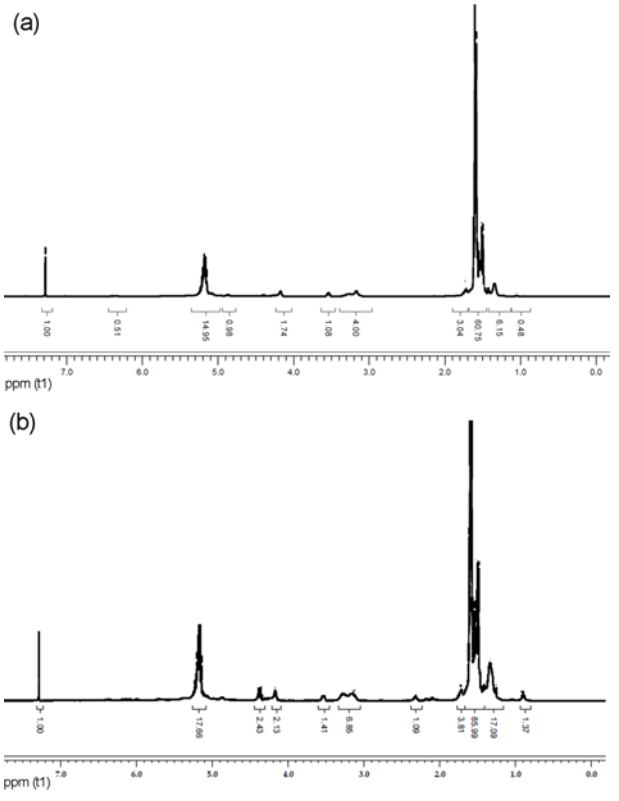

Figure 6. ^{1}HNMR spectrum of (a) P3-100-0 sample and (b) P3-75-25 sample.

The ^{1}HNMR spectrum of P3-100-0 is shown in Figure 6(a). As mentioned before, this sample was HTO-free. By comparing the ^{1}HNMR spectrum of this PU with that of PLA-OH (Figure 2), all characteristic peak shifts belonging to PLA-OH (1.58 and 5.18 ppm which are, respectively, related to methyl and methine protons of the PLA repeating unit) still existed in the PU spectrum, while the shift assigned to the end groups of PLA-OH sample (1.48 and 4.36 ppm in Figure 2) completely disappeared in the PU spectrum. Another point is that the chemical shifts of the butanediol outer protons in the PLA-OH sample (4.17 ppm in Figure 2) were also present in the PU spectrum. Figure 6(b) shows the ^{1}HNMR spectrum of the P3-75-25 sample in which the mole ratio of PLA-OH to HTO was 3 (75 to 25). By adding HTO in the synthesis of PU, the chemical shifts of HTO would appear in PU spectrum. It is clear when comparing the ^{1}HNMR spectrum of P3-75-25 with that of P3-50-50 (Figure 5(b)), the increase of HTO in P3-50-50 resulted in the relative intensities related to HTO to become stronger. Another important issue is that in the samples containing HTO, the characteristic peaks belonging to HTO existed in the synthesized PU.

So, we concluded from the FTIR and ^{1}HNMR results that the chain-extension reaction between PLA-OH and HTO polyols was achieved. Furthermore, the characteristic peaks or chemical shifts related to PLA-OH or HTO polyols still existed in the FTIR and ^{1}HNMR spectrum of the corresponding synthesized Pus; in addition, the more the mole percent of each polyol sample in the PU synthesis, the stronger the relative intensity of the corresponding set of peaks or shifts.

Table 2. Compositions and molecular weights of resulting PU samples

Samples	PLA-OH/HTO (mol%/mol%)	M_n [a] $\times 10^{-4}$ (gr/mol)	M_w [a] $\times 10^{-4}$ (gr/mol)	PDI
PLA-OH	-	-	-	-
P1-100-0	100/0	3.00	7.04	2.35
P1-75-25	75/25	3.71	8.65	2.33
P1-50-50	50/50	3.36	7.78	2.32
P1-25-75	25/75	0.85	2.03	2.39
P2-100-0	100/0	3.24	7.49	2.31
P2-75-25	75/25	4.58	9.89	2.16
P2-50-50	50/50	3.87	9.21	2.38
P2-25-75	25/75	1.06	2.48	2.34
P3-100-0	100/0	4.38	8.95	2.04
P3-75-25	75/25	6.05	10.41	1.65
P3-50-50	50/50	3.23	7.54	2.33
P3-25-75	25/75	1.34	3.09	2.31

[a]Molecular weights determined by GPC.

The molecular weight of the synthesized PUs was investigated by GPC. The results, including number average molecular weight (M_n), weight average molecular weight (M_w), and polydispersity index (PDI), are listed in Table 2.

Thermal Stability Synthesized PUs (TGA and DTG results)

All data from the TGA analysis of PLA-OH and some of the synthesized PUs are shown in Table 3. Figure 7 shows TGA and DTG graphs of a pure PLA-OH sample (having molecular weight of 2200 g/mol); the onset thermal degradation temperature (T_{onset}) of the PLA-OH was around 155 °C and its maximum thermal decomposition took place at around 280 °C. Other information of the pure PLA-OH is summarized in Table 3.

TGA thermographs of the P3 samples are shown in Figure 8(a) and corresponding DTG graphs are shown in Figure 8(b). It can be seen from the Figure and the data listed in Table 3 that T_{onset} of these series of PUs was in the range of 120 to 166 °C, their 5 % degradation temperature ($T_{0.05}$) in the range of 177 to 207 °C, their maximum decomposition rate temperature of the first stage (T_{max1}) in the range of 269 to 277 °C, and their maximum decomposition rate temperature of the second stage (T_{max2}) in the range of 434 to 438 °C. For the P2 samples the above mentioned temperatures are also listed in Table 3. In the graph of some PU samples, there was a small shoulder around 325 °C which is attributed to the decomposition of the urethane groups of the synthesized PUs [36-38].

The Effect of HTO on Thermal Stability

Comparison of the thermal decomposition temperature of the P3 samples with that of the pure PLA-OH sample showed that P3-100-0 sample had a better thermal stability than PLA-OH. However, adding HTO to the PU synthesis formulation made the P3 series less thermally stable, even at low concentrations of HTO. For instance, 25 mol% of HTO

Table 3. Degree of phase separation and hydrogen bonding index of PU samples

Samples	Degree of phase separation	Hydrogen bonding index
P1-100-0	0.39	0.25
P1-75-25	0.40	0.29
P1-50-50	0.37	0.28
P1-25-75	0.34	0.26
P2-100-0	0.40	0.27
P2-75-25	0.42	0.31
P2-50-50	0.39	0.29
P2-25-75	0.37	0.27
P3-100-0	0.38	0.24
P3-75-25	0.41	0.27
P3-50-50	0.36	0.25
P3-25-75	0.33	0.23

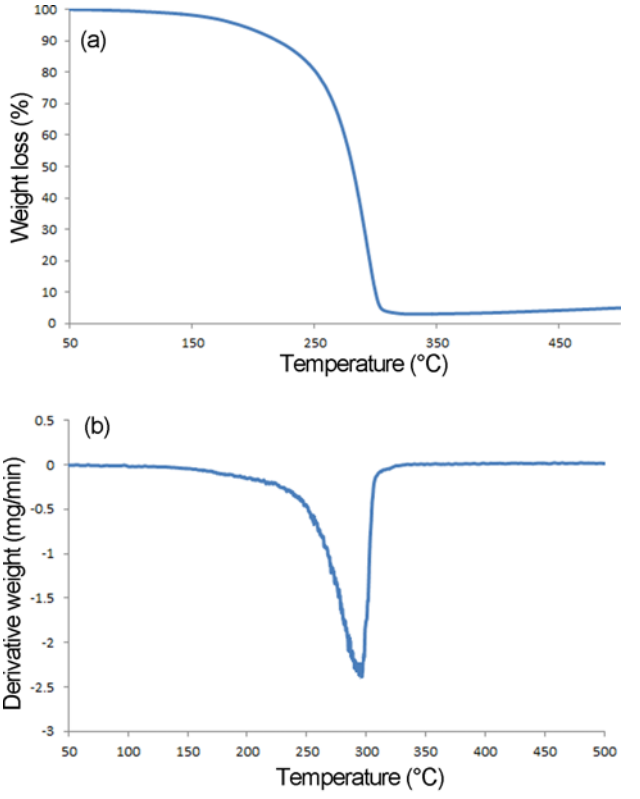

Figure 7. (a) TGA graph of pure PLA-OH sample and (b) DTG graph of pure PLA-OH sample.

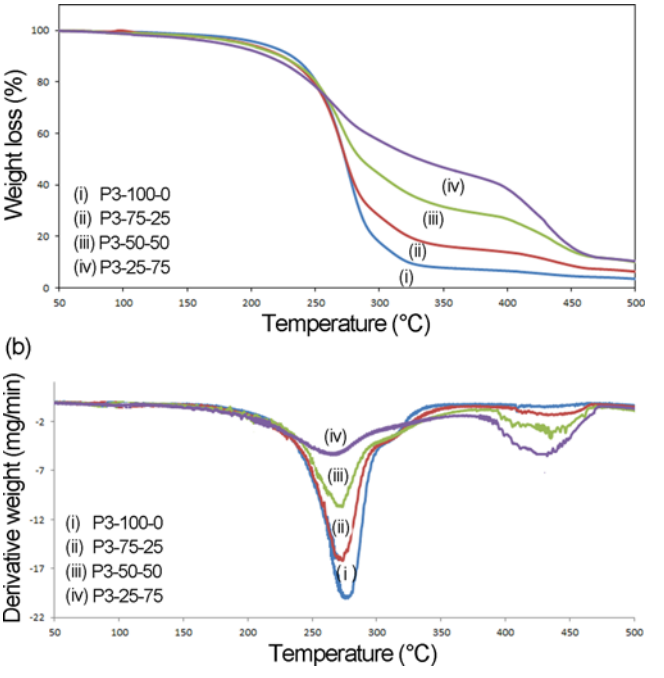

Figure 8. (a) TGA graphs of P3 samples and (b) DTG graphs of P3 samples.

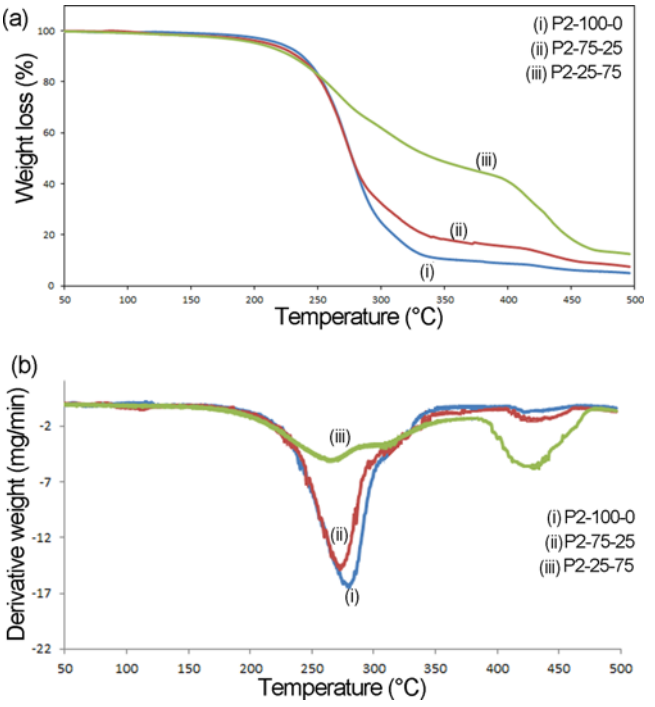

Figure 9. (a) TGA graphs of P2 samples and (b) DTG graphs of P2 samples.

in the formulation of PU caused its onset degradation temperature (T_{onset}) to decrease from 166 °C (P3-100-0) to 145 °C (P3-75-25) which is even less than that of the PLA-OH sample. It seems that the tung oil acted as a plasticizer for the PLA-based PUs and led to a reduced decomposition temperature of PUs. This trend also existed for the P2 series of PUs, in which an increase of HTO in the PU formulation resulted in all decomposition temperatures of PUs becoming lower. It can also be seen from the TGA and DTG graphs of the P2 series, shown in Figure 9, and also from the data in Table 3. However, comparing the rate of weight loss for the P3 or P2 samples in the TGA graphs (Figures 8(a) and 9(a)) and also the ash content at 500 °C (Table 3, last column), showed that the PU samples having HTO in their structures had lower rates of decomposition and more ash content at 500 °C. It is clear from the TGA graphs of the P3 and P2 samples that the samples with higher amount of HTO had lower weight loss in the range of 300-450 °C.

These results showed that, although adding HTO for synthesis of PU caused the decomposition temperature of the synthesized PUs to decrease, the rate of weight loss at higher temperatures for the corresponding PUs became considerably lower in the range of 300-450 °C and also the ash content become greater.

The Effect of PLA-OH Molecular Weight on the Thermal Stability

Another parameter of concern is the molecular weight of the PLA segments. All P2 samples had PLA segments with molecular weight of 1650 g/mol, while the molecular weight of the PLA segments in all of the P3 series was 2200 g/mol. Comparison of the TGA and DTG graphs of P2 and P3 samples showed that almost all degradation temperatures in the P2 samples were higher than those of the P3 samples, and the remaining ash content at 500 °C for the P2 samples was also more than for the P3 samples.

These results showed that the P2 samples were more thermally stable than the P3 samples. The reason for this phenomenon could be related to the hard segment content within the PU chains. In fact, the PLA segments in P2 samples had a molecular weight of 1650, while the ones in the P3 samples had a molecular weight of 2200. So, P2 samples had more hard segments per unit volume of the polymer and these hard segments were more thermally stable than the soft PLA segments; the greater number of hard segments in the P2 series made them more stable. Another reason could be attributed to the longer chain ester of P3 samples. In fact, thermal stability of general esters is not high and because P3 samples have longer chain ester than P2 ones, they were thermally less stable that P2 samples.

The Effect of HTO on the Degradation Mechanism

Another feature is that, considering Figures 8 and 9 for the P2 and P3 samples, adding HTO to PU formulation resulted in appearance of a new peak in TGA or DTG graphs of samples. It was shown for PLA-OH (Figure 7) that its T_{onset} was around 150 °C and its maximum decomposition temperature took place at around 280 °C. For the P2-100-0 and P3-100-0 samples, in which only PLA-OH was the only polyol used for PU synthesis, only one stage of thermal degradation could be seen in the TGA graphs (corresponding to only one peak in the DTG graphs) and no other degradation stage or peak was observable, while for the other P2 and P3 samples, in which HTO was added in the PU synthesis route, another stage of degradation could be recognized in the TGA and DTG graphs (see Figures 8 and 9). So, it could be said that all synthesized PUs underwent a two-stage thermal degradation; the first stage, with a maximum degradation temperature of around 270 °C, is assigned to the PLA segments, and the second stage, with a maximum degradation temperature of around 435 °C, is related to the thermal degradation of the TO segments.

The Effect of PLA-OH Molecular Weight on the Degradation Mechanism

The last feature, the effect of PLA-OH molecular weight on the degradation mechanism is also of concern. Taking into account the DTG graphs of the P2 and P3 samples, it could be seen that the degradation trends for both series of PU samples were similar. Therefore, it could be concluded that the molecular weight of the PLA segment had no effect on the degradation mechanism of PU samples.

Thermal Behavior of the Synthesized PUs (DSC results)

It is well known that thermoplastic polyurethanes show

several thermal transitions because of their soft and hard domains. As researched widely by many authors during the last several decades [39-46], the different endotherms at high temperatures could be attributed to different hard segment ordered structures, dissociation of long range ordering or microphase mixing, and also melting of hard segments rich microphases.

Table 4. Thermogravimetric data of some of the samples

Samples	T_{onset} (°C)	$T_{0.05}$ (°C)	T_{max1} (°C)	T_{max2} (°C)	Ash content at 500 °C (%)
PLA-OH	154	189	279	-	4
P3-100-0	166	207	277	-	4
P3-75-25	145	195	275	440	6
P3-50-50	147	192	274	438	10
P3-25-75	120	177	269	434	10
P2-100-0	189	219	283	-	5
P2-75-25	160	211	277	441	7
P2-25-75	153	203	270	430	12

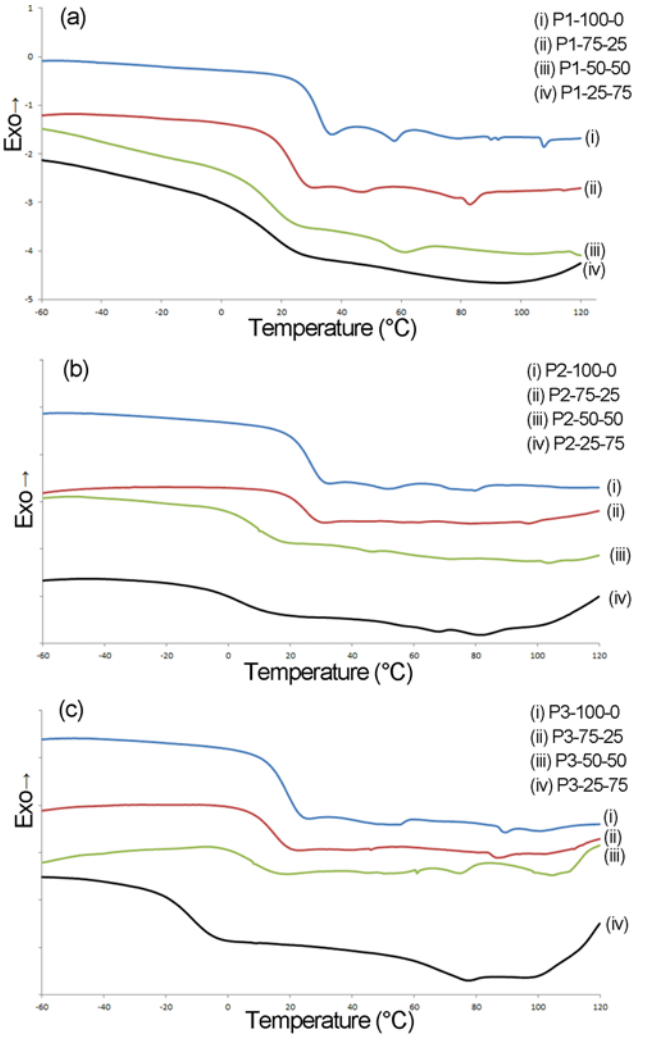

Figure 10. DSC graphs of (a) P1 samples, (b) P2 samples, and (c) P3 samples.

The DSC graphs of the P1, P2, and P3 series of the PU samples are shown in Figures 10(a), 10(b), and 10(c), respectively, and the DSC results are listed in Table 4. For calculation of the degree of crystallinity, the enthalpy of melting for the ideal polymer was assumed equal to the heat of melting of ideally crystalline PLA (94 J/gr) [3]. For each series of synthesized PUs (e.g. the P2 samples, Figure 10(b)), it can be seen that a higher HTO content in the PU formulation led to a lower glass transition temperature of the related PU. This could be attributed to the plasticizing effect of the HTO for the PU. Comparing the graphs of Figures 10(a) to 10(c) shows that the P3 samples had lower glass transition temperatures than the P2 samples, and the P2 samples lower than the P1 samples. In these samples an increase in chain length of the PLA-OH segments resulted in more flexibility of the PU chains. So, it could be concluded that the greater the chain length of the PLA-OH segments, the more the flexibility of the resulting PU chains, and so the lower the glass transition temperature of the final PU samples. This trend did not change significantly with changing molar ratio of HTO for the PU synthesis.

Several endothermic peaks at higher temperatures can be seen in each series of synthesized PUs. The thermal transitions occurring in the 50 to 60 °C region could be assigned to melting of the crystal structures present within the PU structures. Comparison of these peaks for different samples showed that the peak intensity of the P1 samples were greater than those of the P2 samples, and the P2 greater than the P3 ones. This could be due to the greater HS content present inside the synthesized PUs containing PLA-OH of lower molecular weight. Thus, it could be said that greater PLA segment length resulted in less area of the melting peaks (less ΔH_f). Another result could be obtained by comparing the peak intensities of these endotherms with respect to HTO concentration for each series of PU samples. For instance, in Figure 10(a), for the P1 series, greater HTO content in the PU formulation resulted in a decrease of the corresponding peak intensity, in such a way that for P1-25-75 almost no clear peak could be seen. Thus, it could also be concluded that the presence of HTO in the formulation of final PU sample interfered with the formation of hard domains.

Altogether, from all of the above TGA and DSC results, we concluded that lower molecular weight of PLA segment along with less concentration of HTO in the formulation of the final PU sample would lead to a higher glass transition temperature, more HS content, and somewhat a greater thermal stability of the corresponding PU sample.

Evaluation of Side Reactions during PU Synthesis

It is well known that the most important and desirable reaction for the synthesis of a PU is the chain-extension

reaction between two polyols and a chain extender. However, some other side reactions may occur during this reaction [47]. The major side reactions consist of dimerization and trimerization, and carbodiimide, biuret and allophanate formation [48,49]. Furthermore, high temperatures can also increase the crosslink density of the prepolymer through uncontrolled diisocyanate side reactions [50].

In the case of the PU synthesis in our study, a type of aliphatic diisocyanate, i.e. HDI, was used. Aliphatic diisocyanates appear to form dimers only in low yields, while aromatic ones are easily dimerized at low temperatures and both of them can form trimers. Therefore, because we used an aliphatic diisocyanate in our study, the possibility of dimer formation would be very low. The formation of carbodiimide occurs only at very high temperatures, i.e. above 200 °C. Furthermore, the allophanate and biuret formation can take place under a variety of conditions; their contribution would be especially significant at temperatures more than 120 °C [51]. However, considering the temperature range of the reactions used here, it should be noted that the possibility of these side reactions was very low in our study for which the applied temperature was 100 °C. However, we carried out many more experiments to evaluate possibilities of the side reactions during the PU synthesis and the results showed that chain extension reaction was done without any considerable byproducts. However, more experiments were carried out to analyze the presence of side reactions during polyurethane synthesis. The results showed that the chain extension reaction was completely done and the presence of no side reactions was proven experimentally.

Biodegradation Results

Biodegradation tests of the synthesized PUs were carried out using Simulated Body Fluid (SBF). The samples were weighed before and after placing in SBF and the weight losses percent were obtained. Table 5 shows the weight loss of some of the samples. The bar chart of the weight of the samples is shown in Figure 11. As is clear from the chart, the samples had weight loss percents between 0.9 and 10.6. Thus, firstly, it can be concluded that all synthesized PUs were biodegradable and would be degraded when placed in SBF; in other words the physiological liquids of the body would degrade the PU samples and make them lose weight.

Considering the weight losses of the P2 samples and the effect of HTO amount on the weight loss of the samples, it can be seen that sample P2-75-25 (3.6 percent) had a greater weight loss compared to sample P2-50-50 (1.6 percent), and this sample had a greater weight loss than sample P2-25-75 (1.0 percent). So, increasing the mole percent of HTO in preparing the PU polymers (which means decreasing the amount of PLA-OH segment) led to less weight loss of the samples. This result shows that the PLA-OH segments must be the only segments that undergo degradation during this period of time inside the SBF. Therefore, the greater the amount of PLA-OH segments in the PU sample, the more the degradation of the corresponding PU sample and, consequently, the greater its weight loss.

Table 5. DSC results of synthesized PUs

Samples	T_g (°C)	T_{HS1} (°C)	T_{HS2} (°C)	T_{HS3} (°C)	ΔH_m (J/gr)	X_c [a] (%)
PLA-OH	-12.9	70.4	92.2	99.7	- [b]	-
P1-100-0	32.3	57.6	90.9	108.2	11.73	12.5
P1-75-25	23.5	46.9	82.9	113.9	5.52	5.9
P1-50-50	17.3	62.6	-	118.2	4.14	4.4
P1-25-75	16.0	-	93.9	-	-	-
P2-100-0	26.9	51.2	75.9	-	-	-
P2-75-25	25.8	60.3	76.6	96.9	11.96	12.7
P2-50-50	9.96	46.9	-	103.6	9.89	10.5
P2-25-75	4.93	-	67.2	81.6	8.97	9.5
P3-100-0	19.3	55.2	86.5	-	-	-
P3-75-25	14.9	-	87.2	-	-	-
P3-50-50	8.2	51.6	75.9	104.9	8.51	9.1
P3-25-75	-11.6	-	77.5	98.2	4.14	4.4

[a]Enthalpy of melting and degree of crystallinity related to the last peak (T_{HS3}) and [b]not determined.

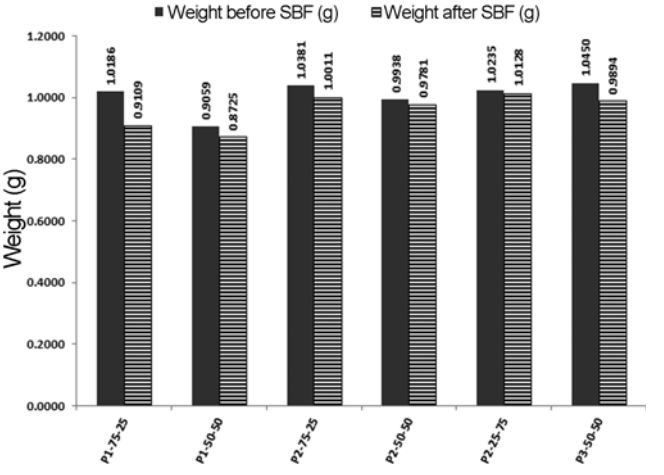

Figure 11. The weight of the samples before and after placing in SBF.

Taking into account the weight loss of samples with equal amounts of PLA-OH and HTO segments (i.e., P1-50-50, P2-50-50 and P3-50-50), it can be seen from Table 5 that the weight loss of P1-50-50 (3.7 percent) was greater than that of P2-50-50 (1.6 percent) and that of P2-50-50 was greater than that of P3-50-50 (0.9 percent). This shows that increase of the molecular weight of PLA-OH segment caused a decrease of the weight loss in the PU sample. In other words, the greater the molecular weight of the PLA-OH segments in the PU sample, the less the biodegradation rate of the PU sample.

Table 6. Weight of some samples before and after placing in SBF

Samples	Weight of sample before SBF (gr)	Weight of sample after SBF (gr)	Weight loss (%)
P1-75-25	1.0186	0.9109	10.6
P1-50-50	0.9059	0.8725	3.7
P2-75-25	1.0381	1.0011	3.6
P2-50-50	0.9938	0.9781	1.6
P2-25-75	1.0235	1.0128	1.0
P3-75-25	1.0119	0.9894	2.2
P3-50-50	1.0450	1.0359	0.9

Therefore, from the biodegradation results, we concluded that the PLA-OH segments were the only segments responsible for biodegradation of the biodegradable polyurethane, and increasing the mole percent of PLA-OH along with its lower weigh will result in less biodegradation of the corresponding polyurethane.

Conclusion

A novel biodegradable polylactic acid-based polyurethane (PU) was synthesized via the chain extension reaction between hydroxylated polylactic acid (PLA-OH) and hydroxylated tung oil (HTO) using 1,6-hexamethylene diisocyanate (HDI) for linking the two polyols together and dibutyltin dilaurate (DBTDL) as a catalyst. Three different molecular weights of PLA-OH prepolymers were used, and the molar ratio of PLA-OH to HTO was also changed to investigate the effect of these parameters on the structure and properties of final PUs. The results showed that the chain-extension reaction of the two polyols with HDI was achieved. Polyurethanes with PLA segments of lower molecular weights were more thermally stable. The results also showed that adding HTO to the PU structure made it considerably softer; in addition, the glass transition temperatures of the PUs having PLA-OH segments with higher molecular weights were lower than those of the PUs having PLA-OH segments with lower molecular weights. It was also concluded that the PLA-OH segments were the only segments responsible for biodegradation of biodegradable polyurethane, and that an increase of its mole percent and also the lower weight of it, would lead to less degradation of the corresponding polyurethane.

References

1. L. S. Nair and C. T. Laurencin, *Prog. Polym. Sci.*, **32**, 762 (2007).
2. S. Singh and S. S. Ray, *J. Nanosci. Nanotechnol.*, **7**, 2596 (2007).
3. M. Mochizuki, *Biopolymers*, **4**, 1 (2002).
4. M. Yamamoto, U. Witt, G. Skupin, D. Beimborn, and R. J. Mueller, *Biopolymers*, **4**, 299 (2002).
5. Y. Choi, S. Y. Kim, S. H. Kim, K. S. Lee, C. Kim, and Y. Byun, *Int. J. Pharm*., **215**, 67 (2001).
6. T. W. Chung, Y. Y. Huang, and Y. Z. Liu, *Int. J. Pharm*., **212**, 161 (2001).
7. K. H. Lam, A. J. Nijenhuis, H. Bartels, A. R. Postema, M. F. Jonkman, A. J. Pennings, and P. Nieuwenhuis, *J. Appl. Biomater.*, **6**, 191 (1995).
8. M. Yoneda, K. Hayashida, K. Izawa, K. Shimada, and K. Shino, *Arthroscopy*, **12**, 293 (1996).
9. S. Vainionpaa, P. Rokkanen, and P. Tormala, *Prog. Polym. Sci.*, **14**, 616 (1989).
10. P. X. Ma, R. Zhang, G. Xiao, and R. J. Franceschi, *Biomed. Mater. Res.*, **54**, 284 (2000).
11. K. Y. Kim and I. J. Chin, *Polym. Prepr.*, **44**, 890 (2003).
12. T. R. Cooper and F. S. Robson, *Macromolecules*, **41**, 55 (2008).
13. J. Borda, I. Bodnar, S. Keki, L. Sipos, and M. Zsuga, *J. Polym. Sci. Pol. Chem*., **38**, 2925 (2000).
14. J. B. Zeng, Y. D. Li, Q. Y. Zhu, K. K. Yang, X. L. Wang, and Y. Z. Wang, *Polymer*, **50**, 1178 (2009).
15. J. B. Zeng, Y. D. Li, W. D. Li, K. K. Yang, X. L. Wang, and Y. Z. Wang, *Ind. Eng. Chem. Res.*, **48**, 1706 (2009).
16. O. Jeon, S. H. Lee, S. H. Kim, Y. M. Lee, and Y. H. Kim, *Macromolecules*, **36**, 5585 (2003).
17. W. Chen, W. Luo, S. Wang, and J. Bei, *Polym. Adv. Technol.*, **14**, 245 (2003).
18. D. Pospiech, H. Komber, D. Jehnichen, L. Haussler, K. Eckstein, H. Scheibner, A. Janke, H. R. Kricheldorf, and O. Petermann, *Biomacromolecules*, **6**, 439 (2005).
19. D. Cohn and A. Hotovely-Salomon, *Polymer*, **46**, 2068 (2005).
20. J. Borda, I. Bodnar, I. Rathy, and M. Zsuga, *Polym. Adv. Technol.*, **14**, 813 (2003).
21. J. Kylma and J. V. Seppala, *Macromolecules*, **30**, 2876 (1997).
22. D. Cohn and A. F. Salomon, *Biomaterials*, **26**, 2297 (2005).
23. E. C. Wood, "Tung Oil: A New American Industry", pp.30-44, U.S. Government Printing Office, Washington, DC, 1949.
24. X. Kong and S. S. Narine in "Industrial and Consumer Nonedible Products from Oils and Fats" (F. Shahidi Ed.), pp.279-281, Wiley, New York, 2005.
25. S. N. Khot, J. J. Lascala, E. Can, S. S. Morye, G. I. Williams, G. R. Palmese, S. H. Kusefoglu, and R. P. Wool, *J. Appl. Polym. Sci*., **82**, 703 (2001).
26. K. S. Chian and L. H. Gan, *J. Appl. Polym. Sci.*, **68**, 509 (1998).
27. A. Guo, I. Javni, and Z. Petrovic, *J. Appl. Polym. Sci.*, **77**, 467 (2000).
28. Y. H. Hu, Y. Gao, D. N. Wang, C. P. Hu, S. Zu, L. Vanoverloop, and D. Randall, *J. Appl. Polym. Sci.*, **84**, 591 (2002).

29. M. A. Corcuera, L. Rueda, B. Fernandez d'Arlas, A. Arbelaiz, C. Marieta, I. Mondragon, and A. Eceiza, *Polym. Degrad. Stabil.*, **95**, 2175 (2010).
30. M. A. Mosiewicki, U. Casado, N. E. Marcovich, and M. I. Aranguren, *Polym. Eng. Sci.*, **49**, 685 (2009).
31. H. Izadi-Vasafi, G. Mir Mohamad Sadeghi, and H. Garmabi, *J. Appl. Polym. Sci.*, **125**, E604 (2012).
32. K. Hiltunen, M. Härkönen, J. V. Seppälä, and T. Väänänen, *Macromolecules*, **29**, 8677 (1996).
33. Y. Tezuka, N. Ishii, K. Kasuya, and H. Mitomo, *Polym. Degrad. Stabil.,* **84**, 115 (2004).
34. K. Hiltunen, J. V. Seppala, and M. Harkonen, *J. Appl. Polym. Sci*., **63**, 1091 (1997).
35. M. M. Coleman, K. H. Lee, D. J. Skrovanek, and P. C. Painter, *Macromolecules*, **19**, 2149 (1986).
36. C. W. Meuse, X. Yang, D. Yang, and S. L. Hsu, *Macromolecules*, **25**, 925 (1992).
37. M. Amrollahi, G. Mir Mohamad Sadeghi, and Y. Kashcooli, *Mater. Des.*, **32**, 3933 (2011).
38. M. V. Pergal, V. V. Antic, M. N. Govedarica, D. Goäevac, S. Ostojic, and J. Donlagic, *J. Appl. Polym. Sci.*, **122**, 2715 (2011).
39. E. G. Bajsic, V. Rek, A. Sendijarevic, V. Sendijarevic, and K. C. Frisch, *J. Elastom. Plast.*, **32**, 163 (2000).
40. R. W. Seymour and S. L. Cooper, *Macromolecules*, **6**, 48 (1973).
41. R. W. Seymour, G. M. Estes, and S. L. Cooper, *Macromolecules*, **3**, 579 (1970).
42. J. T. Koberstein and T. P. Russell, *Macromolecules*, **19**, 714 (1986).
43. J. T. Koberstein, A. F. Galambos, and L. M. Leung, *Macromolecules*, **25**, 6195 (1992).
44. L. M. Leung and J. T. Koberstein, *J. Polym. Sci. Polym. Phys. Ed*., **23**, 1883 (1985).
45. A. Saiani, W. A. Daunch, H. Verbeke, J. W. Leenslag, and J. S. Higgins, *Macromolecules*, **34**, 9059 (2001).
46. A. Saiani, C. Rochas, G. Eeckhaut, W. A. Daunch, J. W. Leenslag, and J. S. Higgins, *Macromolecules*, **37**, 1411 (2004).
47. W. Cooper, R. W. Pearson, and S. Darke, *The Industrial Chemist*, **36**, 121 (1960).
48. S. Gogolewski, *Colloid. Polym. Sci.*, **267**, 757 (1989).
49. Z. S. Petrovic and J. Ferguson, *Prog. Polym. Sci.*, **16**, 695 (1991).
50. H. F. Mark, "Encyclopedia of Polymer Science and Technology", 2nd ed., pp.1988-1990, Wiley-Interscience, New York, 1998.
51. D. J. Lyman, *Rev. Macromol. Chem.*, **1**, 191 (1966).